ELSEVIER

Physica D 129 (1999) 203–222

PHYSICA D

Noise-induced input dependence in a convectively unstable dynamical system

Koichi Fujimoto *, Kunihiko Kaneko

Department of Pure and Applied Science, University of Tokyo, Komaba, Meguro-ku, Tokyo 153-9802, Japan

Received 20 May 1998; received in revised form 24 December 1998; accepted 25 January 1999
Communicated by Y. Kuramoto

Abstract

A uni-directionally coupled dynamical system is studied by focusing on the input (or boundary) dependence. Due to a convective instability, upstream noise is spatially amplified forming downstream oscillations. The resulting downstream dynamics shows both analogue and digital changes, where the former is represented by a change in the oscillation frequency and the latter by a different type of dynamics. The underlying universal mechanism for these changes is clarified by the spatial change of the co-moving Lyapunov exponent which is then used to formulate a condition for the input dependence. The mechanism has a remarkable dependence on the noise strength, and works only in a certain range of the noise amplitude. The relevance of our mechanism to intra-cellular signal dynamics is discussed by considering the correspondences between (a) our dynamics and the auto-catalytic biochemical reactions for the chemical concentration, (b) the input and the external signal, and (c) the noise and the concentration fluctuations of the chemicals. ©1999 Elsevier Science B.V. All rights reserved.

1. Introduction

In biological systems, signaling phenomena which transform external inputs to outputs are important. In general, the signaling process is not simple, and a fixed one-to-one correspondence between the input and output does not exist. A typical example is intra-cellular signaling where several chemicals are involved. These chemicals undergo several catalytic reactions which result in a positive feedback process that amplifies the input. Thus, we are concerned with a nonlinear dynamics of coupled (chaotic) elements.

In a cell, an external stimulus coming from the outside of a cell is selected, amplified, and transported as a signal. Recent developments in molecular biology provide us with more and more detailed information on the signaling process [1]. Experiments in molecular biology have made the mechanisms of chemical signal transmission clearer, while the networks of the pathways by signal chemicals from a given stimulus to the final response have also been clarified.

* Corresponding author. E-mail: fujimoto@complex.c.u-tokyo.ac.jp.

0167-2789/99/$ – see front matter ©1999 Elsevier Science B.V. All rights reserved.
PII: S0167-2789(99)00019-6

A network of signaling pathways is generally rather complicated. A large number of biochemical reactions are involved, from the cell membrane to ligand to the final response reaction. Often, a pathway may not be uni-directional, and several pathways may interfere with each other. With this complication one could even surmise that there is no correlation between the input and the final response. Obviously that would preclude any biological functions. Then, why is the network of signal pathways so long and complicated? How can a signal pathway respond suitably to inputs? How can the signal process work given the possibility of thermodynamic fluctuations?

To answer such general questions, experimental molecular biology alone is not sufficient, and a theoretical study on the general features of biosystems is required. Therefore, we start by studying a simple, uni-directional model pathway as an idealistic simplification of the real signal pathway. We adopt a model where a sequence of biochemical reactions transforms an input into a final response. It is not our aim to construct a biologically realistic model, but what we focus on is the abstraction of an important aspect of the dynamical system by a simple model. In doing so, we will propose a mechanism for the amplification and transmission of signals within fluctuations.

For understanding the mechanism of signaling, we note that the signal system should at least have the following three properties;

Property 1. Amplification and transmission of an input; an external signal is amplified and transmitted through an intra-cellular dynamics.

Property 2. (Linear) stability; the system returns to the original state when the input is off.

Property 3. Input dependence; the response of the system depends on the nature and strength of the input signal.

In the present paper, we introduce an abstract model that consists of a simple biochemical signal pathway, and show that its dynamics has the above three properties. In signal pathways, there are several reaction chains, where, by means of enzyme-catalyzed pathways, many biochemical reactions are driven in one direction through the coupling to energetically favorable hydrolysis of ATP to ADP and inorganic phosphates [1]. Here, a model is introduced with a chain of coupled chemical reactions.

In dynamical systems with one-way coupling, the notion of convective instability is important. i.e. small perturbations are amplified downstreams, even though the system is linearly stable and has a stationary state when there is no such perturbation. We will show that Properties 1 and 2 are closely connected to this convective instability, as will be explained in the next section. It will also be shown that some one-way coupled dynamical systems with convective instability can have Property 3.

Here we consider a catalytic reaction network whose elements are represented by differential equations showing excitatory dynamics. Each element is assumed to be connected uni-directionally. To be specific, we choose the model,

$$\dot{\vec{X}}^i = \vec{F}(\vec{X}^i, \vec{X}^{i-1}) \tag{1}$$

with $\vec{X}^i = (x^i, y^i)$.

In the present model, the input is represented by the boundary condition $\vec{X}^0 = \text{const}$, while the response is given by the dynamics at an downstream site $i \gg 1$. We will find input dependence, or in other words boundary-condition sensitivity, and clarify its mechanism with the help of the notion of convective instability.

Since a convectively unstable (CU) system is often sensitive to noise as described later, it is important to investigate how signal transmission can work in the presence of noise due to chemical fluctuations. Indeed, we will show that our mechanism works in the presence of noise, or rather, that it works best when the noise is of medium strength.

Although our motivation originates in signaling phenomena, our formulation of input-dependent dynamics can generally be applied to any uni-directional chain-type dynamical system. In this respect, the mechanism of analogue and digital input-dependence, as well as our formula for its condition, will have general applicability.

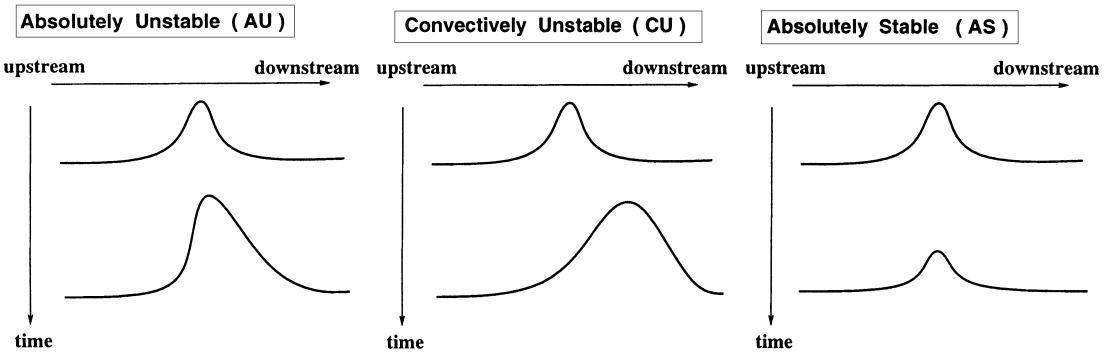

Fig. 1. Schematic representation of the evolution of a perturbation.

It may include neural networks [2], optical networks [3], open fluid flow, and other chain network dynamical systems.

The present paper is organized as follows. In Section 2, noise amplification by convective instability will be reviewed. In Section 3, a simple model using coupled chemical reactions is introduced for biological signaling pathways. In Section 4, the input dependence in our model is presented, while its mechanism will be explained in Section 5 in connection with convective instability and its spatial change due to the input signal. In Section 6, the relevance of noise to the input dependence is described. It is shown that the input dependence is possible only within some range of noise amplitudes. Section 7 is devoted to the discussion and conclusion.

2. Convective instability in a one-way coupled system

2.1. Convective instability

A one-way coupled system was introduced in [4–6] as an abstract model for open flow systems, for example, a fluid system. By spatial amplification of upstream disturbances, the dynamics increases in complexity in the downstream direction [4–10]. This change of dynamics is often triggered by convective instability.

Convective instability expresses how some perturbation is amplified along a flow [4,11–14]. If a system is CU, a perturbation is temporally damped and spatially amplified and transmitted as shown in Fig. 1. On the other hand, if a system is asymptotically stable (AS), an upstream perturbation is damped as it goes downstreams. If a system is absolutely unstable (AU), a perturbation is both temporally and spatially amplified. Note that even if the perturbation is temporally damped at each site, the system can be CU as shown in Fig. 1.

Convective instability is quantitatively characterized by the co-moving Lyapunov exponent λ_v. This is a Lyapunov exponent observed in an inertial system moving with the velocity v [15,16]. If $\max_v \lambda_v$ is positive for a given state, the state is CU. The condition for AS is given by $\max_v \lambda_v < 0$, which is different from the condition $\lambda_0 < 0$ for linear stability. (See Table 1.) The co-moving Lyapunov exponent is usually applied to an attractor where chaos with convective instability is characterized by the positivity of $\max_v \lambda_v$. It can, however, be applied to any state to characterize its stability.

Since λ_v characterizes the amplification of a perturbation for the velocity v, the amplification per one lattice site is given by λ_v/v. Hence the amplification rate per one site is given by the spatial Lyapunov exponent λ^{S} [17];

$$\lambda^{\mathrm{S}} = \max_v \frac{\lambda_v}{v} \tag{2}$$

Table 1
Conditions for absolutely unstable (AU), convectively unstable (CU) and absolutely stable (AS)

	$\max_v \lambda_v$	λ_0
AU	+	+
CU	+	−
AS	−	−

Note that the traditional research of convective instability is focused on a spatially stationary state. To analyze the 'input dependence' in the present paper, the spatial 'inhomogeneity' of convective instability is essential, as will be shown. In Section 5.1, we will introduce a 'local' co-moving Lyapunov exponent to analyze the spatial amplification of a disturbance in a system with spatially inhomogeneous convective instability. With the introduction of new quantifiers, the condition for the occurrence of input dependence can quantitatively be analyzed.

2.2. Noise-sustained structures in a CU system

For a system with convective instability, noise plays an important role. When a system is CU, applied noise is spatially amplified and transmitted from the upstream to the downstream regions of the system until at some stage a spatiotemporal structure is generated [4,10]. This structure is different from that of the noiseless case.

The mechanism of the structure formation can be summarized as follows. Assume that noise is added to a CU-fixed point. Around the fixed point, the noise is spatially amplified and transmitted in the downstream direction. The further downstream it propagates, the larger the oscillation becomes until some stationary dynamics (such as a periodic oscillation) is generated for a certain $i \gg 1$. As long as the noise is added to the most upstream element ($i = 0$), the downstream dynamics remains same. This noise-induced structure in a CU system is a general feature of one-way coupled systems and important for our model. Of course, if the system is AS around the fixed points at all elements, noise is spatially damped, and no downstream structure can be sustained.

3. Model

As a simple signaling model, we choose a system of one-way coupled differential equations (OCDE) [1], where the differential equation at each element can be regarded to express the dynamics of a biochemical reaction.

3.1. Dynamics of a single element

For the dynamics of a single element, we choose an auto-catalytic biochemical reaction system, consisting of an activator x and an inhibitor y (see Fig. 2). In other words, there is a set of two chemical variables for the chemical concentrations, represented by a differential equation with two degrees of freedom.

As a specific example, we choose the following model,

$$\begin{cases} \dot{x} = f(x, y) \\ \dot{y} = g(x, y) \end{cases} \tag{3}$$

with

$$\begin{cases} f(x, y) = x\{(1 - x)ax - by\} + K \\ g(x, y) = y(cx - dy) + K \end{cases} \tag{4}$$

[1] OCDE have also been studied by Aranson et al. [7].

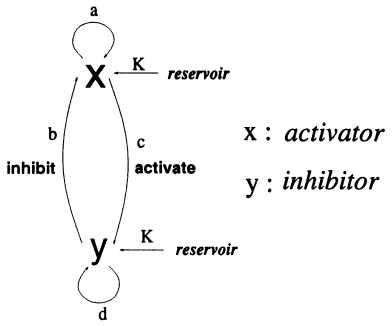

Fig. 2. Schematic representation of the biochemical reaction of a single element.

where the parameters a, b, c, d, and K can be viewed as the rate constants of the biochemical reaction. In the present paper, we set $K \ll 1, a, b, c, d \sim 1$ so that the system has the three properties mentioned in Section 1. In the present case, the suppression of the catalytic process is provided for by the term $(1 - x)$ (where x is between 0 and 1), but other forms like Michael–Menten's can also be adopted [1]. [2]

Note that this single-element dynamics is chosen so that (x, y) converges to a linearly stable fixed point (x_*, y_*), with $f(x_*, y_*) = g(x_*, y_*) = 0$, which has Property 2 in Section 1. There is neither a stable limit cycle nor another fixed point besides the above fixed point.

3.2. One-way coupling

Assuming that the dynamics of each node i is identical, the coupling from one node to the next is introduced as the activation process. In other words, we assume that the activator chemical at the ith node is catalyzed by the $(i-1)$th activator. This leads to the following set of one-way coupled differential equations:

$$\begin{cases} \dot{x}^i = f(x^i, y^i, x^{i-1}) \\ \dot{y}^i = g(x^i, y^i) \end{cases} \tag{5}$$

$$\begin{cases} f(x^i, y^i, x^{i-1}) = x^i\{(1 - x^i)(ax^i + \epsilon x^{i-1}) - by^i\} + K + \eta_x^i \\ g(x^i, y^i) = y^i(cx^i - dy^i) + K + \eta_y^i \end{cases} \tag{6}$$

where i denotes the spatial position or the level of the signal pathway. The coupling constant ϵ corresponds to the rate constant of the biochemical reaction between the $(i-1)$th activator and the ith activator. The concentration fluctuations of the chemicals are represented by the white noise η which satisfies

$$\langle \eta_p^j(t)\eta_q^k(t-\tau)\rangle_t = \delta_{p,q}\delta_{j,k}\delta(\tau)\sigma^2 \tag{7}$$

with σ the i, x and y independent strength of the fluctuations. All the parameters are assumed to be independent of the node i, for simplicity. Again, the details of the coupling form are not important, as long as some nonlinear one-way coupling is included.

This pathway transforms an external signal into a final response. Here, the input signal is given by the concentration x^0 (an external signaling chemical) which appears as a parameter in the dynamics of x^1. This chemical concentration x^0 is set to be constant. The dependence of the downstream response of the concentrations of the chemicals at $(i \gg 1)$

[2] Although a specific model is introduced here, the results generally hold for chain-type excitable systems, and thus, the details of the model are not important.

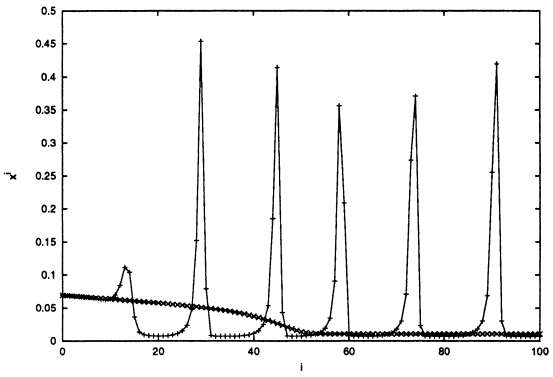

Fig. 3. Snapshots of space-amplitude plots for our system with noise ($+$: $\sigma = 10^{-4}$) and without noise ($\times$: $\sigma = 0$). With noise, the downstream dynamics of each element is periodic. For all the figures in this paper we choose the parameter values: $a = 0.4, b = 5.12, c = 2.0$, $d = 3.55$, $K = 0.0004$, $\epsilon = 2.8$.

on the value of x^0 is studied. In other words, x^0 works as the boundary condition of the one-way coupled system. In the present paper, we do not consider its temporal change (like an input oscillation), although its introduction will be an interesting problem for future consideration.

With regards to the connection to cell signaling problems, the node i can be regarded either as corresponding to a one-dimensional spatial position in a cell or as corresponding to a level of kinase–kinase. . . . reaction. In the latter case, the use of identical reactions for all the nodes i is, of course, too drastic a simplification. Still, it is useful to discuss a possible signaling mechanism in this simple case. Indeed the mechanism and concepts presented in this paper can straightforwardly be applied even if the reaction equation is different for each element i.

3.3. Numerical results: pulse generation

As mentioned, all elements converge to a fixed point for all initial and boundary conditions, when no noise is added as shown in Fig. 3. The boundary dependence of the upstream spatial pattern (x_i^*, y_i^*) of fixed points rather rapidly disappears in the downstream direction, and (x_i^*, y_i^*) quickly approaches (x^*, y^*). The downstream pattern is spatially constant and its value does not depend on the input.

Here we are interested in the case that the fixed point pattern is CU at least at some point. Then the mechanism mentioned in Section 2.2 works when some noise is added. We have found that a pulse-like downstream oscillation is generated as shown in Fig. 3 (see also Fig. 4). Often (i.e. for most parameter values and input values), the generated oscillation is periodic, with the downstream oscillation becoming periodic both in space and time. In other words, the pulse is transmitted in the downstream direction changing its pattern (i.e., its amplitude or frequency).[3] Note that the limit cycle has to be AS to be transmitted in the downstream direction without being changed by noise added at each element. Still, this limit cycle disappears if the noise is turned off.

4. Input dependence

To investigate the input dependence of the pulse-like solution, we have changed the concentration x^0 and studied how the downstream dynamics responds. Here the boundary (input) concentration is taken to be fixed in time, and the temporal information of the input is discarded.

[3] Of course, there are fluctuations around the periodic oscillation due to the noise. Still, this fluctuation decreases as $i \to \infty$ if the noise is applied only at $i = 0$. Hence we call the dynamics a 'periodic oscillation,' even though it is triggered by stochastic fluctuations.

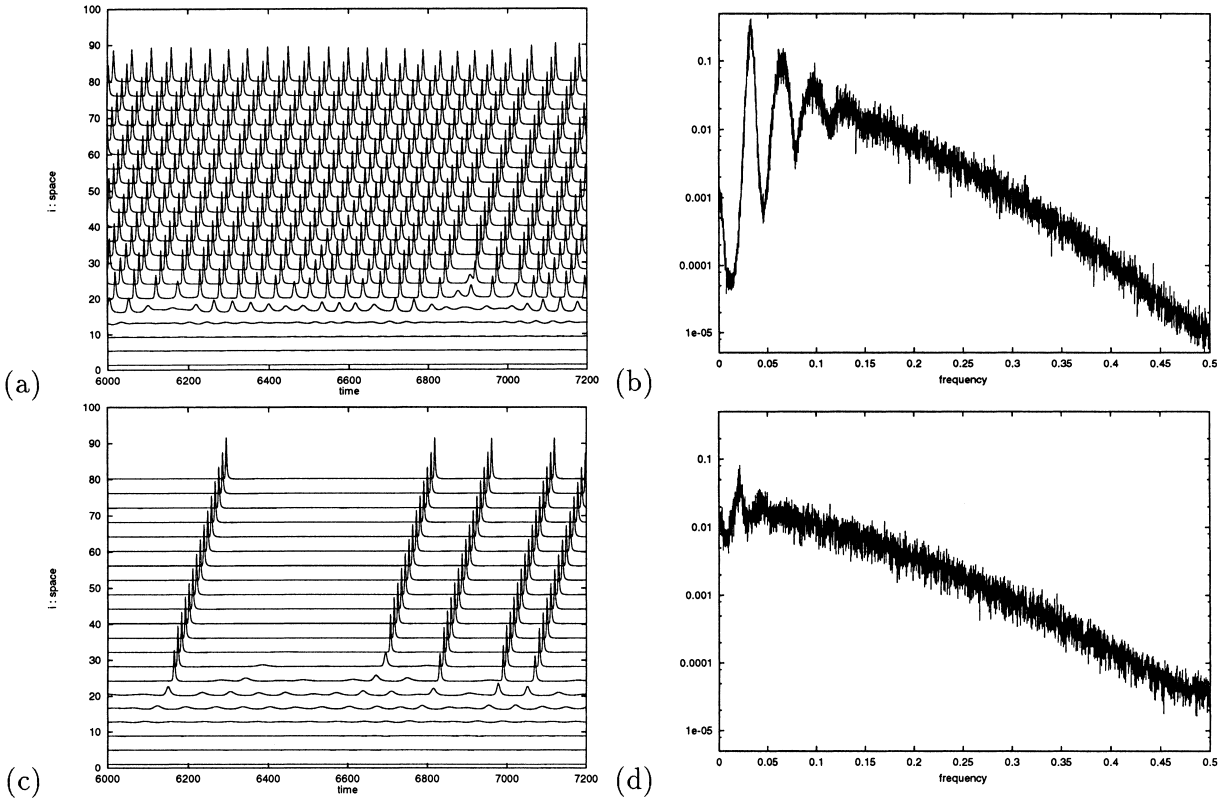

Fig. 4. Spatiotemporal plot of $x^i(t)$ (a, c) and the corresponding power spectrum (b, d) with $i = 80$. The input values x^0 are 0.070 (a, b) and 0.054 (c,d). (a) and (b) show periodic oscillations at downstream nodes, (c) and (d) show stochastic oscillations. $\sigma = 1.0 \times 10^{-4}$. The parameters a, b, c, d, K, ϵ are the same as in Fig. 3.

Two types of input dependence are discovered as regards the downstream dynamics, given by the behavior of $(x^i(t), y^i(t))$ at $i \gg 1$. The first type of input dependence is 'digital' (i.e., threshold-dependent), represented by different types of dynamics, such as fixed points, oscillation, and so forth, while the second type of input dependence is 'analogue,' in the sense that the frequency or amplitude of the oscillation changes. Note that these input dependences of the downstream dynamics are kept even for $i \to \infty$ where the dynamics converges spatially.

4.1. Digital dependence

With the application of noise to all elements, the downstream dynamics shows the following three phases successively with the increase of the input value (the boundary condition) x^0. The difference of the phases is shown in Fig. 4 where the spatiotemporal pattern and the corresponding power spectrum of the time series of a downstream node x^i are depicted.

4.1.1. Periodic oscillation phase (p-phase)

At downstream nodes, periodic oscillations with large amplitudes are generated, as shown in Fig. 4(a). The downstream motion is quite regular in the presence of noise, as is shown in the power spectrum of x^i for $i = 80$ (see Fig. 4(b)). The orbit of (x^i, y^i) is plotted in phase space in Fig. 5. Note that the orbit does not pass through the fixed point of the noiseless case.

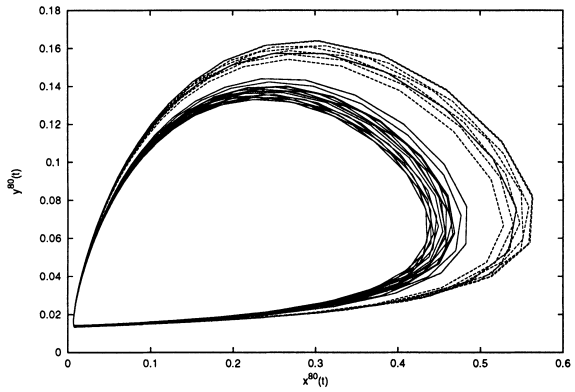

Fig. 5. Phase space at $i = 80$ for different input values x^0. The parameters a, b, c, d, K, ϵ, and the intensity of the noise σ are same as in Fig. 4. The dotted line corresponds to Fig. 4(c) (stochastic oscillation), while the solid line corresponds to Fig. 4(a) (p-phase).

As mentioned in Section 3.2, when the noise is turned off, the oscillation damps and each element's dynamics converges to a fixed point. On the other hand, the oscillation is AS and transmitted without being influenced by noise.

Stochastic oscillation regime: Around the onset of the p-phase, stochastic oscillations with a large amplitudes are generated at downstream nodes. The intervals between the peaks are stochastic and much longer than the periods in the p-phase (see Fig. 4(c) for the spatiotemporal pattern). The amplification and transmission of noise occurs only stochastically in the present phase, in contrast with the regular transmission. Peaks in the power spectrum of the downstream dynamics are no longer observed, as shown in Fig. 4(d), and are replaced by broad band spectra. The orbit stays close to the fixed point of the noiseless case for a long time, emits a pulse train stochastically once, and then returns to the previous fixed point. (See Fig. 5 where the orbit of (x^i, y^i) is plotted.)

Although the oscillation is aperiodic, each pulse itself remains AS and is transmitted without being influenced by the noise.

4.1.2. Fixed point phase (f-phase)

No pulse is generated, and the orbit stays around the fixed points with some fluctuations ($\sim \sigma$). No spatial amplification is observed. At the transition from the p-phase to the present phase, the frequency of the pulse generation goes to zero.

We have measured the distribution of the intervals between the peaks of downstream x^i as the boundary x^0 is varied. In the p-phase, the distribution has a sharp peak, while in the stochastic oscillation regime there is no peak and the distributions becomes broader.

To investigate whether the dynamics converges downstreams, we have measured the variance of x, that is $\langle (x^i)^2 \rangle - \langle x^i \rangle^2$, with $\langle \dots \rangle$ the temporal average. Fig. 6 gives the spatial change of the variance for three different boundary conditions x^0. The upper plot corresponds to the p-phase, the middle one to the stochastic regime, and the bottom one to the f-phase. As can be seen in the figure, the dynamics converges spatially around $i \sim 30$, while the input dependence is preserved for $i \to \infty$. (Indeed we have confirmed that the variance $\langle (x^i)^2 \rangle - \langle x^i \rangle^2$ remains different for each boundary condition.) All of our results indicate that the input dependence is not a special transient but a lasting response for $i \to \infty$.

4.2. Analogue dependence

The analogue dependence on the input is characterized by a continuous change of the frequency and amplitude of the oscillation (at $i \gg 1$) when varying the input, i.e, the boundary condition x^0. It is observed both in the

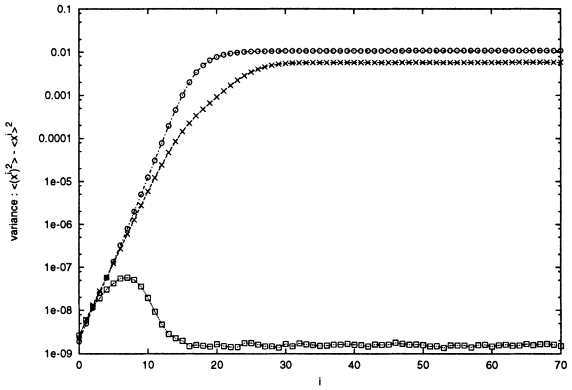

Fig. 6. Dependence of the variance $\langle (x^i)^2 \rangle - \langle x^i \rangle^2$ on the site i. The top line ($\circ$) corresponds to the input of Fig. 4(a) (p-phase), the middle line ($\times$) to Fig. 4(c) (stochastic oscillation regime), and the bottom line ($\square$) corresponds to the fixed point phase (f-phase). The dynamics spatially converges around $i \sim 30$ and the input dependence remains for $i \to \infty$. The parameters a, b, c, d, K, ϵ, and the intensity of the noise σ are the same as in Fig. 4.

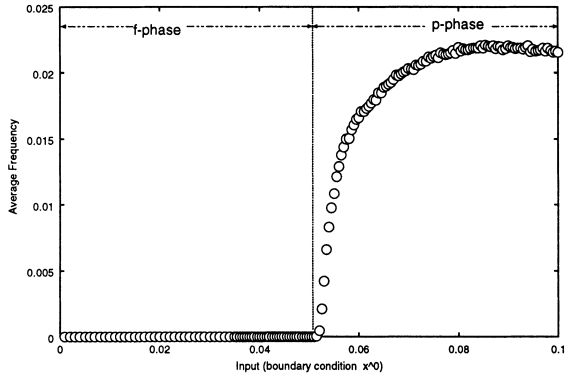

Fig. 7. The input dependence of the average frequency of pulses at downstream nodes is plotted. From the power spectrum, we find that the p-phase lies around $x^0 > 0.051$ (while the stochastic oscillation regime lies around $0.054 > x^0 > 0.051$). For both the regimes, the average frequency changes with the input value x^0. The parameters a, b, c, d, K, ϵ, and the intensity of the noise σ are same as in Fig. 4.

periodic and stochastic oscillation regimes. Fig. 7 shows the input dependence of the average frequency of the downstream dynamics. In both regimes, the average frequency of the downstream dynamics changes continuously with the boundary value x^0. The downstream dynamics shows not only digital but also analogue dependence on the boundary. We have also measured the power spectrum of the downstream dynamics. The position of the peak frequency (and hence the response dynamics) continuously changes with the input x^0.

5. Mechanism

How is the input dependence formed? Recall the following two properties described in Section 2.2: First, the formation of a pulse train structure depends on whether the fixed point solution is AS or CU. Second, the nature of the generated oscillation is influenced by the degree of the convective instability of the fixed point in the region where the pulse is being formed.

By referring to these properties, the mechanism of the input dependence can be sketched as follows: depending on the input value x^0, the fixed point values of the upstream nodes change, resulting in a change of the degree of

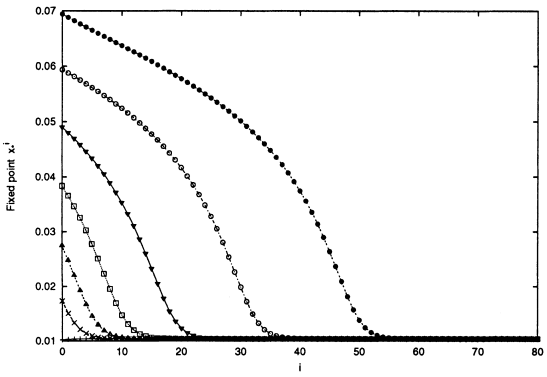

Fig. 8. The fixed point $x_*(i)$ is plotted for different input values x^0. The parameters a, b, c, d, K, ϵ are the same as in Fig. 4. Different marks correspond to different input values, $x^0 = 0.01\,(+)$, $0.02\,(\times)$, $0.03\,(\triangle)$, $0.04\,(\square)$, $0.05\,(\triangledown)$, $0.06\,(\circ)$, and $0.07\,(\bullet)$.

convective instability. Accordingly the spatial amplification rate of the noise changes, and the generated downstream dynamics can be different. In this section, we study the above mechanism of the input dependence in terms of the convective instability of the fixed point.

Without noise, all elements converge to fixed points (x_*^i, y_*^i) which depend on the site i. We now would like to introduce the site-dependent co-moving Lyapunov exponent $\lambda_v(i)$, and the spatial instability exponent $\lambda^{\mathrm{S}}(i)$ of (x_*^i, y_*^i). We will see that the input dependence can be explained by the spatial change of $\lambda^{\mathrm{S}}(i)$.

5.1. Spatial convergence of fixed points

In our model, (x_*^i, y_*^i) is determined as follows:

$$\begin{cases} \dot{x}_*^i = f(x_*^i, y_*^i, x_*^{i-1}) = 0 \\ \dot{y}_*^i = g(x_*^i, y_*^i) = 0 \end{cases} \tag{8}$$

Eq. (8) is a recursive equation from (x_*^{i-1}, y_*^{i-1}) to (x_*^i, y_*^i). Given x^0 at the left boundary, this equation can be solved successively for $i = 1, 2, \ldots$ by the iteration. The trace of the spatial convergence, $(x_*^1, y_*^1) \to (x_*^i, y_*^i) \to (x_*^\infty, y_*^\infty)$ is determined as in Fig. 8. In our model, (x_*^∞, y_*^∞) can be determined uniquely[4] for $\forall x^0$. We use the notation,

$$\begin{aligned} &(x_*, y_*) \equiv (x_*^\infty, y_*^\infty) \\ &\lambda_*^{\mathrm{S}} \equiv \lambda_*^{\mathrm{S}}(\infty) \end{aligned} \tag{9}$$

Now let us study the convective instability of this fixed point. Since the fixed point is site dependent, we extend the concept of the co-moving Lyapunov exponent to a spatially local quantifier by measuring the amplification of a perturbation to the next site from each site for a given velocity. Technically this amplification rate is measured as the co-moving Lyapunov exponent of a snapshot homogeneous pattern $(x^l, y^l) = (x_*^i, y_*^i)$ for $l \geq i$ (see Appendix A).

Fig. 9(a) shows the co-moving Lyapunov exponent $\lambda_v(i)$ of the fixed point at each site, while $\lambda_v(i)/v$ of the fixed point at each site is shown in Fig. 9(b). Here, the site dependence can clearly be seen. At $i \leq 30$ the fixed point is CU, since $\lambda_v(i)$ is positive at $v \sim 0.1$. On the other hand, at $i \geq 30$, the fixed point is AS, and $\lambda_v(i)$ is negative for all v. In our model, the fixed points change from convectively unstable to absolutely stable ones in the downstream direction.

[4] It is an interesting future problem to study a case with multiple solutions for (x_*^∞, y_*^∞)

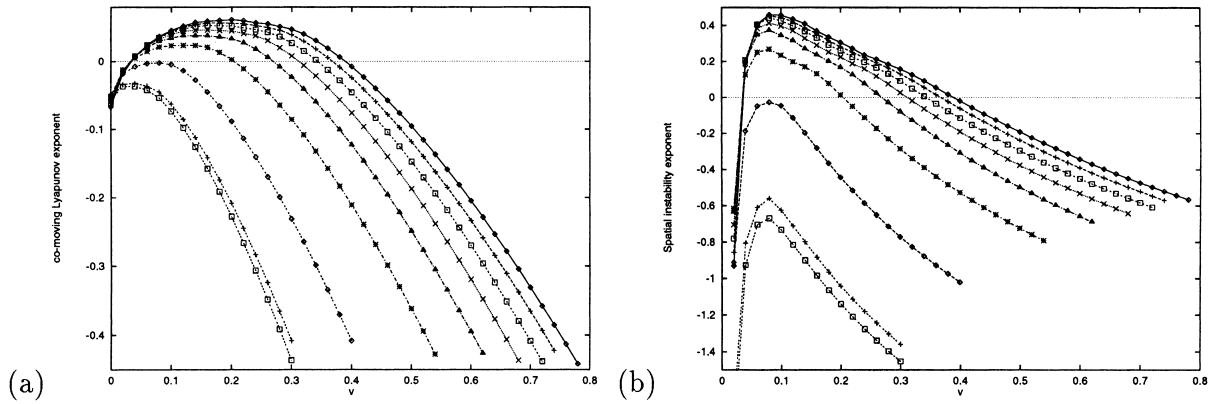

Fig. 9. Co-moving Lyapunov exponents $\lambda_v(i)$ (a), and the spatial instability exponents $\lambda_v(i)/(v)$ (b) are plotted as a function of v, for $i = 0\,(\diamond), 5\,(+), 10\,(\square), 15\,(\times), 20\,(\triangle), 25\,(*), 30\,(\diamond), 35\,(+), 40\,(\square)$, from the top to bottom. The parameters a, b, c, d, K, ϵ are the same as in Fig. 4. The boundary condition is given by $x^0 = 0.060$. $\lambda_v(i)/v$ attains its maximum at $v \sim 0.1$ for every site.

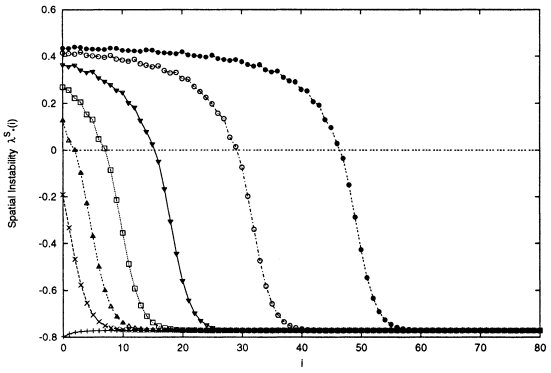

Fig. 10. Spatial instability exponent $\lambda_*^{\mathrm{S}}(i)$ of fixed points. Different marks represent different input values, $x^0 = 0.01\,(+), 0.02\,(\times), 0.03\,(\triangle), 0.04\,(\square), 0.05\,(\triangledown), 0.06\,(\circ)$, and $0.07\,(\bullet)$, corresponding to Fig. 8.

Table 2
Composition of AS or CU states at upstream and downstream sites

	Fixed point at upstream	Fixed point at downstream	Limit cycle at downstream
Type 1	AS	AS	None
Type 2	CU	AS	AS
Type 3	CU or AS	CU	AS

Recall that the growth rate of a perturbation to the next site is given by the spatial instability $\lambda^S(i) = \max_v(\lambda_v(i)/v)$. In our model, the velocity v which maximizes $\lambda_v(i)/v$ is independent of i, as is shown in Fig. 9(b). The dependence of $\lambda^{\mathrm{S}}(i)$ on the input x^0 is shown in Fig. 10. In our model, the relaxation is monotonic (either decreasing or increasing) for $\lambda_*^S(i)$ to λ_*^S as $i \to \infty$ [5].

Now we discuss the relationship between $\lambda_*^{\mathrm{S}}(i)$ and the input dependence. In Table 2, we have classified our dynamics into three types according to the convective instability at upstream and downstream sites.

[5] It is interesting to study a case with a non-monotonic convergence of fixed points (such as a spatially periodic or chaotic case) in the future.

First, for Type 1, no oscillation is generated, since the fixed point is AS. The fixed point approaches a constant value for $i \to \infty$, and the state value of the downstream sites is input independent. For Type 3 the downstream fixed point is CU, and spatial amplification from a fixed point always occurs, independently of the input value x^0. Hence, no digital change occurs. Indeed, in numerical simulations, a digital change from a fixed point to an oscillatory regime is observed only in the Type 2 case. In this case, there are two AS states for $i \to \infty$ in the presence of noise. One is the fixed point (x_*, y_*) and the other one is a limit cycle. Depending on the nature of the upstream dynamics, one of the two states is selected. This leads to a digital change in the dynamics.

5.2. Mechanism of the digital change

In this section the mechanism of the digital change is quantitatively analyzed in terms of the co-moving Lyapunov exponent.

Since the fixed point becomes absolutely stable for downstream sites, the oscillatory dynamics should be formed before the fixed point has stabilized. Hence the condition for the formation of oscillatory dynamics is given by the competition between two length scales. The scale i_u where the lattice remains CU, and the 'growth scale' i_g, where perturbations grow, a requirement for the generation of pulses. The scale i_u is given by the site where the fixed point (x_*^i, y_*^i) becomes AS. In other words, $\lambda^{\mathrm{S}}(i) > 0$ at $i < i_u$ and $\lambda^{\mathrm{S}}(i) < 0$ at $i > i_u$.

The scale i_g can be estimated as the scale where the noise is amplified to O(1). As long as the noise is small, the amplification rate of the noise is determined by the spatial instability $\lambda_*^{\mathrm{S}}(i)$ of the fixed point (x_*^i, y_*^i). Hence i_g can roughly be estimated as follows:

$$\sigma \prod_{i=0}^{i_g} \mathrm{e}^{\lambda_*^{\mathrm{S}}(i)} = \sigma \mathrm{e}^{\sum_{i=0}^{i_g} \lambda_*^{\mathrm{S}}(i)} \sim 1 \tag{10}$$

Hence,

$$\sum_{i=0}^{i_g} \lambda_*^{\mathrm{S}}(i) \sim \log \frac{1}{\sigma} \tag{11}$$

Since the perturbation is no longer amplified in an AS state, it is necessary that the noise is amplified at sites that are CU. The noise has to be amplified to O(1) before $i \sim i_u$. Thus, the condition $i_g \lesssim i_u$ is imposed in order to have oscillatory dynamics. As the input (boundary) changes, the fixed points (x_*^i, y_*^i) change accordingly, and both i_u and i_g change. Then the relation between i_g and i_u can change qualitatively. Fig. 11 shows the input dependence of i_g and i_u for our model for parameters belonging to the Type 2 regime. Note that the relationship $i_g \lessgtr i_u$ depends on the input value x^0. For $x^0 > 0.065$, i_g is smaller than i_u, and indeed we have observed oscillatory dynamics with a large amplitude. Around $x^0 \sim 0.065$, $i_g \sim i_u$, and stochastic oscillations are found with intermittent pulse generation from the fixed point state. No pulse is generated for $x^0 < 0.065$.

We can summarize the changes in the dynamics according to the relationship between i_g and i_u as follows (see Fig. 12):

- $i_g < i_u$: This is the *periodic phase* where a stationary oscillation is formed at downstream sites. Since the generated oscillation itself is AS, the pulse is transmitted downstreams without being affected by noise. As long as the noise is added stationarily (at least at upstream sites), a spatially stationary downstream state is formed. The stochastic oscillation regime is seen around $i_g \sim i_u$, where the formation of the pulse is strongly sensitive to noise. The formed pulse itself is AS and can be transmitted in the downstream direction stationarily, but its formation is intermittent. Indeed, we have measured i_u / i_g for various parameters in the stochastic phase, and the value stays around $1.0 \sim 1.2$.

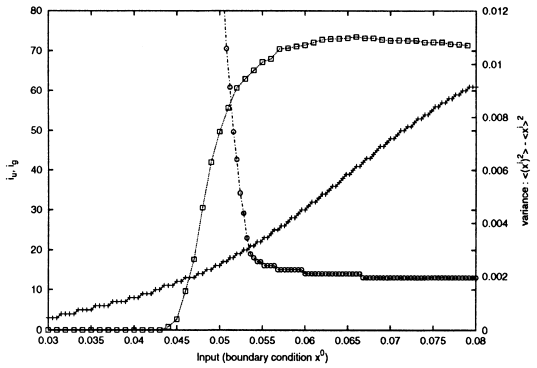

Fig. 11. Dependence of i_u (+) and i_g (○) on the input value x^0. For reference, the variance of x^{80} (□) is also plotted. The parameters a, b, c, d, K, ϵ are the same as in Fig. 4. The intensity of the noise is $\sigma = 0.001$.

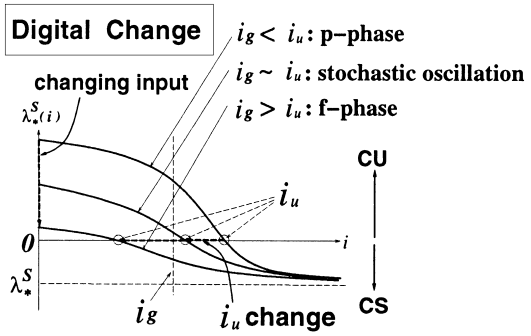

Fig. 12. Schematic diagram of the change of λ_*^S in each of the three phases.

- $i_g = \infty$ ($i_g > i_u$): This is the *fixed point phase* where the fixed point becomes AS before a pulse is generated. No pulse exists, and the downstream dynamics remains near the fixed point with some noise. Indeed, condition Eq. (10) is not satisfied for any finite i_g.

It should be noted that the above mechanism generally holds for one-way coupled systems where the fixed points are convectively unstable in the upstream region and absolutely stable in the downstream region. This also clarifies why the digital change is found only in the Type 2 regime. In the Type 1 regime, i_u is ∞, and only the fixed point phase appears, while in the Type 3 regime, i_u is zero, and the pulse is formed irrespective of the boundary condition (input).

5.3. Mechanism of the analogue change

Here we discuss the input dependence of the response frequency. The formation rate of the pulse is expected to depend on the convective instability of the fixed points before the pulse train is formed. On the other hand, if the fixed point approaches (x_*, y_*), the spatial instability is independent of the input. Hence, only if the scale i_g, required to form the pulse, is smaller than the scale of the above convergence, the generated downstream dynamics is expected to depend on the input.

As a simple measure of the relaxation length i_r of the fixed points, we will introduce a 'half-decay' scale. Since the spatial convergence of $\lambda_*^S(i)$ is monotonic as described in Section 5.1, and since $\lambda_*^S(i)$ characterizes the amplification of noise, we use the convergence of $\lambda_*^S(i)$ for defining i_r. As the half-decay scale of $\lambda_*^S(i)$, i_r is defined by the site

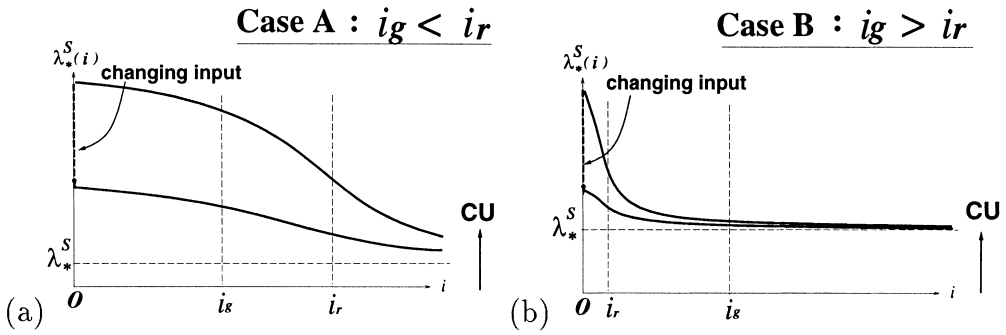

Fig. 13. Schematic diagram of the analogue change. Cases with a clear analogue change (a), and without (b).

which satisfies $\lambda_*^S(i_r) = (\lambda_*^S + \lambda_*^S(0))/2$. Roughly speaking, $\sum_j^i \lambda_*^S(i)$ is sensitive dependent on i for $i < i_r$, while for $i > i_r$, it weakly depends on i. This is expected, for example, when $\lambda_*^S(i)$ exponentially relaxes to λ_*^S.

Now let us focus on the relationship between i_g and i_r. If the convergence scale i_r is much smaller than i_g, the amplification rate of the noise, given by $\sum_j^i \lambda_*^S(j)$, depends little on the input. On the other hand, if i_r is larger than i_g, the amplification rate strongly depends on the input. Since the amplification rate changes continuously with the input value, an analogue change in the response is expected. Hence we have the following two cases:

Case A: $i_g < i_r$: In the region where the pulse is formed ($i < i_g$), the spatial convergence of the fixed points is not yet completed, and the noise amplification rate is dependent on the input. Thus, the nature of the generated wave at $i \sim i_g$ depends on the input. Since the formed wave pattern is stable, this dependence on the input is preserved for downstream sites.

Case B: $i_g > i_r$: Since the fixed point has almost converged to (x_*, y_*) at the site where the wave pattern is formed, the amplification of the noise and the nature of the formed wave are insensitive to the input value. Hence the nature of generated wave depends little on the input.

In order to formulate a condition for the analogue dependence in the Type 2 regime, we need to add a condition for the formation of the wave (discussed in Section 5.2), while in the Type 3 regime the wave is always formed. Hence the conditions for the analogue dependence on the input are summarized as:

$$\begin{cases} \text{Type 2} : (i_g < i_r) \cap (i_g \lesssim i_u) \\ \text{Type 3} : i_g < i_r \end{cases} \tag{12}$$

In Fig. 13 the above mechanism of the analogue change is shown schematically.

Note again that our mechanism for input dependence is universally applicable to one-way coupled dynamical systems, irrespective of the choice of model. In our model, the analogue change is in the frequency of the oscillations. This transformation of input to frequency can be model-specific. In general, there may be a variety of ways in which the transformation of input values to analogue downstream information can take place. Still the argument presented here is applicable to each case.

6. The effect of noise on the input dependence

In the previous section, the mechanism of the input dependence is explained with the help of the spatial change of $\lambda^S(i)$. In this section, the mechanism of the input dependence is discussed from a different angle by investigating the relation between convective instability and noise (fluctuation) intensity. It will be shown that the input dependence is found only for some range of the noise intensity.

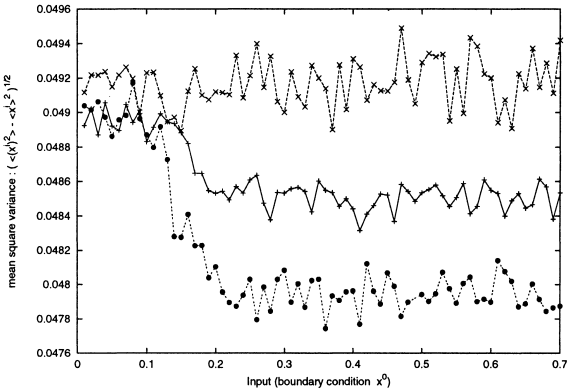

Fig. 14. The mean square variance $(\langle (x^i)^2 \rangle - \langle x^i \rangle^2)^{1/2}$ is plotted against the change of input values for three different values of the noise amplitude. $+ (\sigma = 1.0 \times 10^{-7}) \rightarrow \bullet (\sigma = 3.0 \times 10^{-3}) \rightarrow \times (\sigma = 8.0 \times 10^{-2})$. The parameters correspond to the Type 3 regime, $a = 2.7$, $b = 10.7$, $c = 4.8$, $d = 9.4$, $K = 0.015$, $\epsilon = 4.5$.

Fig. 14 shows our numerical results for the input dependence of the variance of $x^i(t)$ at a downstream site for various noise amplitudes. The parameters are fixed such that the system falls into the Type 3 regime. It can be seen that the mean square variance has input dependence only for noise with a medium intensity ($\bullet$). If the intensity of the noise is too large ($\times$), the variance does not show input dependence, while the dependence becomes weaker as the noise amplitude is decreased ($+$). A 'suitable' range of the noise intensity is required for obtaining the analogue change.

6.1. *Disappearance of the input dependence in a low noise regime*

The mechanism of the disappearance of the input dependence in a low noise regime can straightforwardly be explained with the argument of the previous section. According to Eq. (11), i_g becomes larger when the noise decreases, and the relationship between i_g and i_u or i_r changes. With the decrease of σ, the following two changes are possible.

1. Disappearance of the digital change (in the Type 2 regime): When decreasing σ for a fixed input, i_g becomes larger than i_u, and a transition from the periodic to the fixed point phase occurs. For small σ, the periodic phase no longer appears irrespective of the input values (within their allowed range in our model). Hence the digital dependence on inputs disappears.

   Fig. 15(a) shows the input dependence of the variance of $x^i(t)$ at a downstream site with the change of the noise amplitude, while in Fig. 15(b) the input dependence of i_g and i_u is plotted. As can be seen, the digital change requires larger input values when the noise amplitude is decreased.
2. Disappearance of the analogue change (in either the Type 2 or 3 regime): With the decrease of σ, i_g increases until it becomes larger than i_r, and a change from Case A to Case B in Section 5.3 follows. Thus, the analogue dependence on the input fades out.

The lower limit for the noise σ_S which allows for the input dependence to exist can straightforwardly be estimated from the above argument. The noise intensity must satisfy

$$i_g < \begin{cases} i_r & \text{(analogue change)} \\ i_u & \text{(digital change)} \end{cases} \tag{13}$$

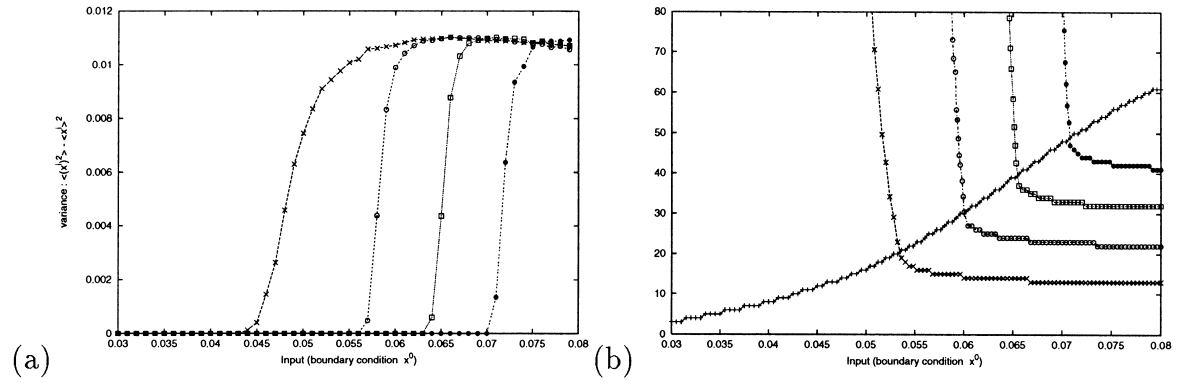

Fig. 15. The input dependences of the variance at $i = 80$ (a), and of i_u (+) and i_g (b) are plotted. The noise amplitudes are $\sigma = 10^{-3}$ (×), 10^{-5} (○), 10^{-7} (□), 10^{-9} (●) for each of the figures (note that i_u does not depend on σ). The smaller the noise amplitude is, the harder it is for the periodic phase to appear within the allowed range of inputs. The parameters a, b, c, d, K, ϵ are the same as in Fig. 4.

By introducing the average spatial instability $\overline{\lambda_*^S} = (1/i_g)\sum_i^{i_g} \lambda_*^S(i)$, and using the expression (11) for i_g, we obtain

$$\sigma > \sigma_S = \begin{cases} \exp(-\overline{\lambda_*^S} i_r) & \text{(analogue change)} \\ \exp(-\overline{\lambda_*^S} i_u) & \text{(digital change)} \end{cases} \tag{14}$$

6.2. Collapse of the input dependence under strong noise

The collapse of the input dependence under strong noise is due to a different mechanism. When the noise intensity is too large, the wave, once formed, can be destroyed due to the noise at downstream sites [6]. The generated oscillation is distorted by the noise, and the downstream transmission does not work well. In particular, in the Type 2 regime, due to the convective instability of the fixed point at downstream sites, the dynamics can stay near the fixed point after the collapse of the limit cycle. Thus, the input dependence of the periodic and fixed point states fades out. There is an upper limit of the noise intensity σ_L where the input dependence disappears. (This upper limit σ_L cannot be estimated with the help of the convective instability of the fixed point. It is a nonlinear effect of the noise around the limit cycle oscillation. In spite of some effects on the nonlinear convective instability [18], no theory is available for the present case so far.)

7. Discussion and conclusions

In the present paper we have reported a boundary (input) dependence in a one-way coupled differential equation, and presented a general mechanism for it. It is shown that this boundary dependence is caused by a spatially dependent convective instability and by noise.

Boundary condition dependence has also been studied in dissipative structures [19]. However, our boundary condition dependence is clearly different from earlier studies. The most important difference is dependence on the system size. The boundary condition dependence studied previously is nothing but a finite size effect. The dependence disappears when the size becomes larger. On the other hand, our boundary condition dependence is not

[6] The noise here plays the same role as that added to an information channel in information theory.

due to such a finite size effect. It remains even in the infinite size limit. The difference in the dynamics, created by a difference in the boundary (input), is fixed to a downstream element i and is maintained even in the limit $i \to \infty$. Also, it should be noted that our boundary dependence is independent of the initial conditions, and is stable against perturbations.

Furthermore, our mechanism supporting the boundary dependence is novel, and should be distinguished from that in the previous studies. In our case, it originates in the spatial amplification of fluctuations by the convective instability, which is in contrast with the use of linear stability in the earlier studies [19]. The amplification rate of the fluctuations, characterized by the (local) convective Lyapunov exponent $\lambda_v(i)$, depends on space, and accordingly on the boundary (input). After amplification, the dynamics stabilizes in the downstream direction. Once stabilized, the dynamics stays as an attractor. The dynamics generated before the spatial convergence can depend on the boundary. On the other hand, the generated difference in the downstream dynamics cannot be changed any more and is fixed due to the stable dynamics there. Hence the boundary dependence is fixed for downstream sites.

We have shown that there are two types of boundary (input) dependence. One is a threshold-type (bifurcation-like, digital) change, leading to a qualitative difference in the downstream dynamics. In our model, this corresponds to a bifurcation from the fixed point to a stable stochastic oscillation, and then to a stable periodic oscillation. The other is a continuous (analogue) change in downstream dynamics. In our example, the frequency of the pulses can continuously change.

These two types of boundary dependence are quantitatively analyzed by introducing three characteristic length scales based on the local convective Lyapunov exponent $\lambda_v(i)$. The first one is the length scale i_g necessary for the fluctuations to be amplified to a macroscopic order of magnitude. The second is the length scale i_u where the convective instability of the fixed point disappears. The third is the length scale i_r characterizing the spatial convergence of $\lambda_v(i)$.

For the bifurcation-like change, it is crucial that the amplification of a fluctuation is completed before the fixed point becomes AS. Otherwise, the downstream dynamics remains at the fixed point. Thus, the condition for the qualitative (digital) change is determined by $i_g \leqslant i_u$. On the other hand, the analogue change depends on whether the amplification is completed while the spatial dependence of the convective instability is significant, and thus, subjected to the condition $i_g \lessapprox i_r$. Note that these conditions also imply that the boundary dependence can be found only within some range of the noise amplitude σ, because $i_g \propto \log \sigma$ from Eq. (11).

Deissler [20] reported for the Ginzburg–Landau equation that the downstream dynamics depends on the length of the convectively unstable upstream region i_u, where a parameter in the model is varied with the spatial position such that the upstream dynamics is convectively unstable and the downstream dynamics absolutely stable.

In our study, in contrast, the parameters are spatially uniform, and the convective instability changes with the position spontaneously, following the relaxation from the boundary condition. Our mechanism for the change of convective instability and the formation of waves may be more relevant, for example, to an open fluid flow without nonuniformity in parameters.

Since our mechanism is expressed in universal terms for dynamical systems, the input (boundary) dependence is expected to be observed generally in spatially extended dynamical systems, as long as a spatially inhomogeneous convective instability exists. It is interesting to search for such a boundary dependence in open-fluid flow [14], optical systems [3], coupled map lattices [5,9], and so forth, and to check whether the relationships between i_g, i_u and i_r are satisfied.

Our motivation for this study originates in biological signaling problems. Then what implications are drawn from our results for such problems?

In our study the input information is represented by the boundary value, while the response is given by a state of the downstream dynamics. In the region $i \lessapprox i_g$ required for the wave formation, the input difference is amplified by the convective instability. The information in the dynamics in this region is translated into a response through

the site-dependent $\lambda_v(i)$. If the conditions for i_g, i_u, and i_r are satisfied, the input information (concentration x^0) can be translated to an output information (dynamics) through the chemical dynamics along the signaling pathway.

Now let us return to the questions raised in Section 1. The first question is regarding the reason for the length and complication of the signaling pathway. According to our mechanism, we need several sites (larger than i_g and i_u) to have input dependence. This number of sites depends on the parameters, but cannot be too small, as long as the dynamics is not too convectively unstable. Hence the pathway must be sufficiently long in order to have input dependence. Of course the signal pathway does not consist of a single chain of reactions, but several chains are mutually interdependent. It is expected that the chain becomes longer 'effectively' by the interaction among multiple chains.

The second question 'how can a system respond suitably to inputs' is answered by the above translation of input (boundary) to response (downstream dynamics) through the spatially dependent convective instability $\lambda_v(i)$. In particular, the digital (bifurcation-like) dependence provides a response with some input threshold, while the analogue dependence provides a translation from an input concentration to a response frequency. Both the dependences are essential to neural and sensory responses. It is also interesting to note that our signal transmission mechanism is different from that given by the Hodgkin–Huxley equation for neural signal transmission [21].

The third question on the robustness of a signaling mechanism under thermodynamic fluctuations is most clearly answered by our mechanism. Indeed our input dependence works in the presence of noise, or rather the noise amplitude σ has to satisfy $\sigma_L > \sigma > \sigma_S$. Note that noise is inevitable in a cell system by thermal fluctuations, and also due to a relatively small number of signaling molecules. Indeed the number of most signal molecules is around $N \sim 1000$. Thus, a noise in the order $1/\sqrt{N} \sim 0.03$ should exist. The condition $\sigma_L > \sigma > \sigma_S$ for the input dependence may be part of the explanation for why most cell response works only within some temperature range, and works in a system with a small number of (signaling) molecules.

Of course several studies need to be carried out in the future, not only in the context of dynamical systems research, but also with regards to the application of our viewpoint to biological signaling phenomena. The following list is currently under investigation.

1. Extension to a case where $\lambda_v(i)$ has complex spatial dynamics: In our model $\lambda_v(i)$ monotonically relaxes to $\lambda_v(\infty)$. In general, the relaxation can be oscillatory or have a chaotic transient, as is found in a one-way coupled map lattice (OCML) [22]. In such a case, a complex input dependence may be expected.
2. Extension to a case with a bi-directional or symmetric coupling: Although the present uni-directional coupling provides a very straightforward example for investigating convective instability, such instability also exists in the bi-directional coupling case, and is characterized by the co-moving Lyapunov exponent $\lambda_v(i)$ [16]. Indeed some preliminary studies show that a boundary condition dependence of our type also exists in systems with bi-directional couplings.
3. Extension to a system with several AS attractors at $i \to \infty$: In this case the selection of an attractor can depend on the input. A complicated dependence on input values may exist similarly to the fractal or riddled basin structures prevalent in multiple attractor systems.
4. Extension to a non-constant input (boundary): If the boundary oscillates in time, for example, this temporal information of the input (boundary) can be translated into a response dynamics. Indeed, in an OCML [9], the input oscillation is selectively transmitted to downstream sites depending on its period.
5. Extension to a multiple chain system with multiple inputs: In a signaling process in a cell, several interacting pathways exist. With multiple boundary values (inputs), a new type of boundary dependence can be expected, such as a response depending on a combination of several inputs.

Acknowledgements

The authors are grateful to T. Yomo, T. Shibata, and I. Tsuda for stimulating discussions. They are also grateful to F. Willeboordse for a critical reading of the manuscript. The work is partially supported by Grant-in-Aids for Scientific Research from the Ministry of Education, Science, and Culture of Japan.

Appendix A. Calculation of the local co-moving Lyapunov exponent of the fixed point (x_*^i, y_*^i)

Since the values of the fixed points are site dependent in our model, the conventional method [8] for calculating the co-moving Lyapunov exponent has to be extended. To measure the amplification rate of a perturbation at a site i, we consider a system where $(x^j, y^j) = (x_*^i, y_*^i)$ for $j \geq i$, and compute the amplification rate per lattice point. Let us consider the evolution equation,

$$\dot{\vec{z}}^j(t) = \vec{h}^j(\vec{z}^j(t),\ \vec{z}^{j-1}(t)) \tag{A.1}$$

with $\vec{h}^j(\vec{z}^j, \vec{z}^{j-1}) = (f(\vec{z}^j, \vec{z}^{j-1}), g(\vec{z}^j, \vec{z}^{j-1}))$.

The displacement follows the equation

$$\delta\dot{\vec{z}}^j(t) = \frac{\partial \vec{h}^j(\vec{z}^j, \vec{z}^{j-1})}{\partial \vec{z}^j}\delta\vec{z}^j(t) + \frac{\partial \vec{h}^j(\vec{z}^j, \vec{z}^{j-1})}{\partial \vec{z}^{j-1}}\delta\vec{z}^{j-1}(t) \tag{A.2}$$

We solve the equation for $\vec{z}^j = (x_*^i, y_*^i)$ for $j \geq i$ and $\forall t$ with the initial condition $\delta\vec{z}^j(0) = \delta_{0,j}\delta$. The solution can be written as

$$\delta\vec{z}^j(t) \equiv J^j(t)\delta\vec{z}^0(0) \tag{A.3}$$

where

$$\dot{J}^j(t) = \frac{\partial \vec{h}^j(\vec{z}^j, \vec{z}^{j-1})}{\partial \vec{z}^j} J^j(t) + \frac{\partial \vec{h}^j(\vec{z}^j, \vec{z}^{j-1})}{\partial \vec{z}^{j-1}} J^{j-1}(t) \tag{A.4}$$

Here, $J^j(t)$ is a 2×2 matrix, and is obtained by solving Eq. (A.4) for the initial condition $\delta\vec{z}^j(0) = \delta_{0,j}\delta$. By defining $e^{\Lambda_1^j(t)}$ and $e^{\Lambda_2^j(t)}$ as absolute values of the eigenvalues of $J^j(t)$ $(\Lambda_1^j(t) \geq \Lambda_2^j(t))$ we obtain

$$\lambda_v(i) \equiv \lim_{t\to\infty} \frac{1}{t}\Lambda_1^j(t)\,\big|_{j=vt} \tag{A.5}$$

References

[1] B. Alberts, D. Bray, J. Lewis, M. Raff, K. Roberts, J.D. Watson, Molecular Biology of the Cell, Garland Publishing, 1994.
[2] I. Tsuda, H. Shimizu, Self-organization of the dynamical channel, in: H. Haken (Ed.), Complex Systems – Operational Approaches, Springer, Berlin, 1985, pp. 240–251.
[3] K. Otsuka, K. Ikeda, Cooperative dynamics and functions in a collective nonlinear optical element system, Phys. Rev. A 39 (1989) 5209–5228.
[4] R.J. Deissler, One-dimensional strings, random fluctuations, and complex chaotic structures, Phys. Lett. A 100 (1984) 451–454.
[5] K. Kaneko, Spatial period-doubling in open flow, Phys. Lett. A 111 (1985) 321–325.
[6] R.J. Deissler, External noise and the origin and dynamics of structure in convectively unstable systems, J. Stat. Phys. 54 (1989) 1459–1488.
[7] I.S. Aranson, A.V. Gaponov-Grekhov, M.I.Ravinovich, The onset and spatial development of turbulence in flow systems, Physica D 33 (1988) 1–20.
[8] J.P. Crutchfield, K. Kaneko, Phenomenology of spatiotemporal chaos, in: B.L. Hao (Ed.), Directions in Chaos, World Scientific, Singapore, 1987, pp. 272–353.

[9] F.H. Willeboordse, K. Kaneko, Pattern dynamics of a coupled map lattice for open flow, Physica D 86 (1995) 428–455.
[10] R.J. Deissler, Noise-sustained structure, intermittency, and the Ginzburg–Landau equation, J. Stat. Phys. 40 (1985) 371–395.
[11] R.J. Briggs, Electron-stream Interaction with Plasmas, MIT Press, Cambridge, MA, USA, 1964.
[12] A. Bers, Space-time evolution of plasma instabilities – absolute and convective, in: M.N. Rosenbluth, R.Z. Sagdeev (Eds.), Handbook of Plasma Physics 1, Elsevier Science, 1983, pp. 451–517.
[13] E.M. Lifshitz, L.P. Pitaevskii, Physical Kinetics, Pergamon, Oxford, 1981.
[14] P. Huerre, Spatio-temporal instabilities in closed and open flows, in: E. Tirapegui, D. Villaroel (Eds.), Instabilities and Nonequilibrium Structures, Reidel, Dordrecht, 1987, pp. 141–177.
[15] R.J. Deissler, K. Kaneko, Velocity-dependent Lyapunov exponent as a measure of chaos for open flows, Phys. Lett. A 119 (1987) 397–402.
[16] K. Kaneko, Lyapunov analysis and information flow in coupled map lattice, Physica D 23 (1986) 436–447.
[17] D. Vergni, M. Falcioni, A. Vulpiani, Spatial complex behavior in nonchaotic flow systems, Phys. Rev. E. 56 (1997) 6170–6172.
[18] J.M. Chomaz, Absolute and convective instabilities in nonlinear systems, Phys. Rev. Lett. 69 (1992) 1931–1934.
[19] G. Nicolis, I. Prigogine, Self-organization in Nonequilibrium Systems, Wiley, 1977, pp. 131–140.
[20] R.J. Deissler, Turbulent bursts, spots and slugs in a Ginzburg–Landau equation, Phys. Lett. A 120 (1987) 334–340.
[21] A.L. Hodgkin, A.F. Huxley, A quantitative description of membrane current and its application to conduction and excitation in nerve, J. Physiol. 117 (1952) 500–544.
[22] K. Fujimoto, K. Kaneko, in preparation.